A R C H I V E S O F M E T A L L U R G Y A N D M A T E R I A L S
Volume 60 2015 Issue 2
DOI: 10.1515/amm-2015-0128

W.H. LEE*, C.S. HONG**, S.Y. CHANG**,♯

EFFECT OF HEAT-TREATMENT ON MICROSTRUCTURE AND MAGNETIC PROPERTIES OF NANOCRYSTALLIZED Mn-Zn FERRITE POWDERS

WPŁYW OBRÓBKI CIEPLNEJ NA MIKROSTRUKTURĘ I WŁAŚCIWOŚCI MAGNETYCZNE NANOKRYSTALICZNYCH PROSZKÓW FERRYTU Mn-Zn

The initial ferrite powders were subjected to high energy ball milling at 300rpm for 3h, and subsequently heat-treated at 573-1273K for 1h. Based on the observation of microstructure and measurement of magnetic properties, the heat-treatment effect was investigated. The size of initial powders was approximately 70μm. After milling, the powders with approximately 230nm in size were obtained, which were composed of the nano-sized particles of approximately 15nm in size. The milled powders became larger to approximately 550nm after heat-treatment at 973K. In addition, the size of particles increased to approximately 120nm with increasing temperature up to 973K. The coercivity of initial powders was almost unchanged after milling, whereas the saturation magnetization increased. As the heat-treatment temperature increased, the saturation magnetization gradually increased and the maximum coercivity was obtained at 773K.

Keywords: High energy ball milling, Nano-sized particles, Crystalline size, Magnetic properties

1. Introduction

Mn-Zn ferrite core has been widely used in electronic applications such as transformers, choke coils, noise filters, recording heads and high-frequency powder electronics, etc [1] because of high intial permeability, high saturation magnetization, low eddy current and low coercivity [2]. It has been also used in biomedicine as magnetic carriers for bioseparation, enzymes and proteins immobilization [3]. Recently, with the development of wireless power transmission, it has been applied for not only small home appliance and battery charger of mobile device but industrial distribution transfer system because of advantage in massive power transfer.

The Mn-Zn ferrite core can be generally fabricated by powder metallurgy processing. In particular, the characteristics of the powders are very important to produce high magnetic performance Mn-Zn ferrite core [5]. It is also well known that the soft magnetic properties could be improved in ultra-fined alloy or nanocrystalline alloy [6]. Among powder metallurgy processing, the high energy ball milling is an effective technique currently used in inorganic materials synthesis to obtain the nano-sized grains [7, 8, 9].

In this study, therefore, the aim is to investigate the microstructure and magnetic properties of the Mn-Zn ferrite powders prepared by the high energy ball milling and subsequently heat-treated at different temperatures.

2. Experimental

In this study, the mixing ferrite powders composed of Fe_2O_3, Mn_2O_3 and $MnZnFe_2O_4$ oxides were used as the initial powders for high energy ball milling, which were analyzed for 38.1 wt% O, 34.3 wt% Fe, 14.6 wt% Mn, 7.2% Zn and 5.8% C elements. It was charged with stainless ball into jars of high energy ball mill. The ball to powder weight ratio was 20:1 and the milling rate was 300rpm. The powders were milled for 3h under argon atmosphere. The milled powders were collected in the glove box filled with argon gas, and subsequently heat-treated at different temperatures ranging from 573K to 1273K for 1h under argon atmosphere.

The microstructure of the powders was characterized by a scanning electron microscope (SEM, JSM-7001F, JEOL, JAPAN) and a transmission electron microscope (TEM, JEM2100F, JEOL, JAPAN). The powder size and shape were investigated by an image analysis. X-ray diffraction (XRD, D/MAX 2500H, RIGAKU, JAPAN) was conducted to determine the phases. The mean crystalline size of the phases was calculated by Debye-Scherrer's equation using the half-value width of peaks [10]. The magnetic properties of the powders were measured at room temperature using a vibrating sample magnetometer (VSM, VSM-5-10, TOEI INDUSTRY, JAPAN).

3. Results and discussion

The typical SEM photographs of initial ferrite powders, milled ferrite powders and heat-treated ferrite powders are shown in Fig. 1. The initial ferrite powders were spherical in shape, whereas the milled powders and heat-treated powders had irregular shape. After milling, the size of initial powders obviously decreased. However, after heat-treatment, the milled powders became slightly larger.

* DEPARTMENT OF ADVANCED MATERIALS ENGINEERING, SEJONG UNIVERSITY, SEOUL 143-747, KOREA
** DEPARTMENT OF MATERIALS ENGINEERING, KOREA AEROSPACE UNIVERSITY, GYEONGGI-DO, 412-791, KOREA
♯ Corresponding author: sychang@kau.ac.kr

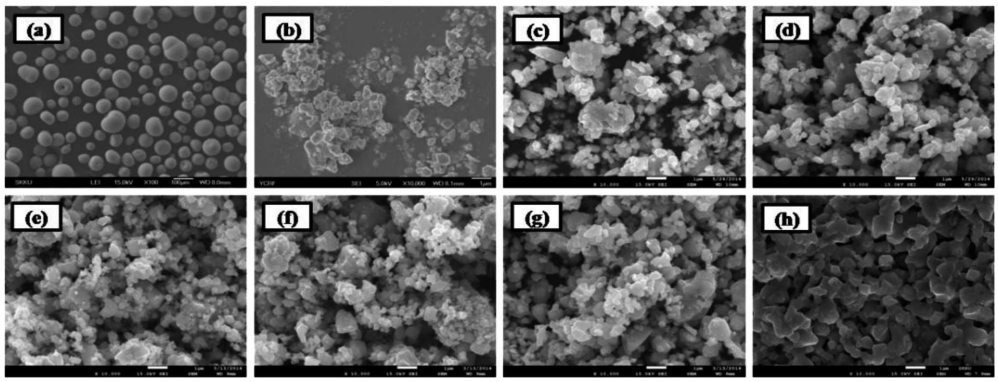

Fig. 1. SEM images showing initial ferrite powders (a), milled powders at 300rpm for 3h (b) and heat-treated powders at 573K (c), 673K (d), 773K (e), 873K (f), 973K (g) and 1273K (h) for 1h

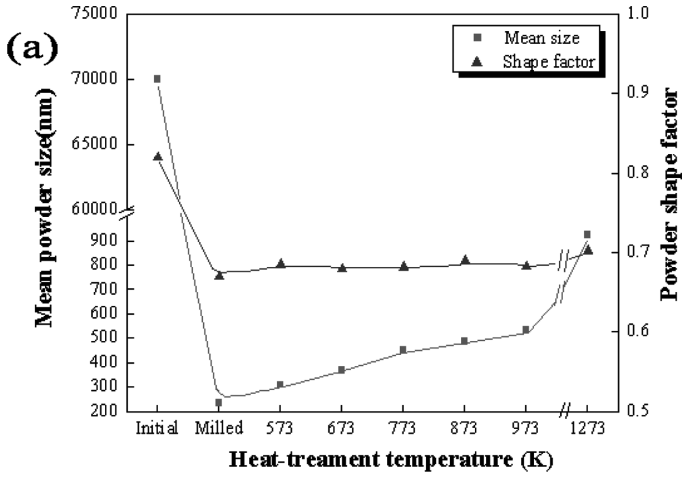

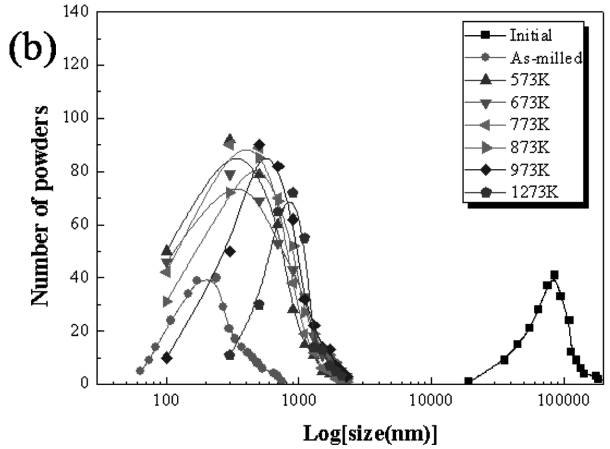

Fig. 2. The mean size and shape factor of powders with heat-treatment temperature (a) and size distribution curves of the initial, milled and heat-treated ferrite powders (b)

The size, shape factor and size distribution of powders obtained from Fig. 1 are quantitatively shown in Fig. 2. The initial ferrite powders had the mean powder size of approximately 70 μm. After milling at 300rpm for 3h, the size of powders was reduced to approximately 230nm. However, it increased after heat-treatment and continuously increased with increasing temperature. At 1273K, the size of powders was increased to approximately 900nm and a distinctly diffused structure was observed. The shape factor of initial ferrite powders was more than 0.8, indicating that the powders were almost sphere. After milling, however, the milled powders had the shape factor of less than 0.7, and it was unchanged after heat-treatment. The size distribution of initial ferrite powders was inbetween 20 and 200 μm. It moved to 60-700nm after milling and gradually moved to right again as the heat-treatment temperature increased. The highest number peak of powders well corresponded to the average size of powders.

Fig. 3 shows TEM photographs of milled ferrite powders and heat-treated powders at different temperatures ranging from 573 to 973K for 1h. It is obvious that the milled ferrite powders and heat-treated ferrite powders shown in Fig. 1 were composed of the nano-sized particles and the growth of particles occurred with increasing temperature.

The mean particle size obtained from Fig. 3 is quantitatively plotted in Fig. 4. The particle size of as-milled powders was approximately 15nm. As the heat-treatment temperature increased, the size of particles increased and it was approximately 120nm at 973K.

Fig. 5 shows XRD patterns of the initial, milled powders and heat-treated powders. The peaks of Fe_2O_3, Mn_2O_3 and $MnZnFe_2O_4$ phases detected in the initial ferrite powders remained after milling. As the heat-treatment was carried out, the Mn_2O_3 and Fe_2O_3 phases decomposed at temperature higher than 773K and 973K, respectively. However, only $MnZnFe_2O_4$ phase formed at 1273K.

Fig. 6 reveals the effect of the heat-treatment temperature on the mean crystalline sizes of the Fe_2O_3, Mn_2O_3 and $MnZnFe_2O_4$ phases calculated by Debye-Scherrer's equation. The crystalline sizes of Fe_2O_3 and Mn_2O_3 phases showed approximately 80 and 90nm at 573K, respectively. As the heat-treatment temperature increased, the crystalline sizes of the Fe_2O_3 and Mn_2O_3 phases decreased and disappeared at 973K and 773K, respectively. This is considered to be due to the decomposition of Fe_2O_3 and Mn_2O_3 phases as the XRD results shown in Fig. 5. In addition, the $MnZnFe_2O_4$ phase had a tendency to decrease size until 773K. At higher temperatures than 773K, however, the $MnZnFe_2O_4$ phase increased in size. Based on XRD result showing the peaks of $MnZnFe_2O_4$ phase, it can be considered that the generation of $MnZnFe_2O_4$ phase could occur continuously until 773K, and then it began to enlarge with increasing temperature.

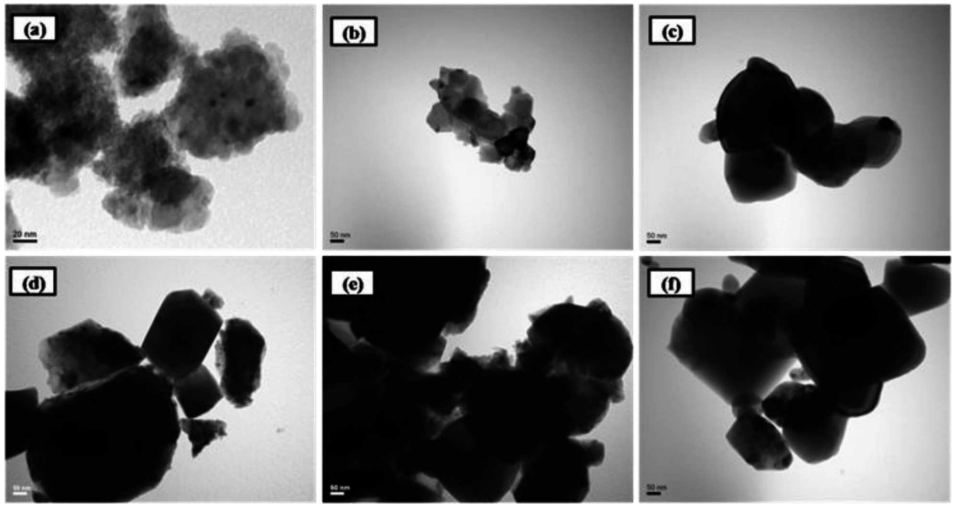

Fig. 3. TEM images showing ferrite powders milled at 300rpm for 3h (a), heat-treated at 573K (b), 673K (c), 773K (d), 873K (e) and 973K (f) for 1h

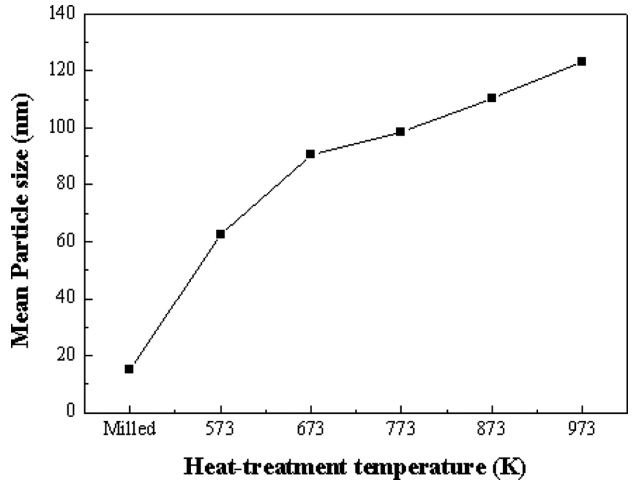

Fig. 4. Change of mean particle size with increasing heat-treatment temperature

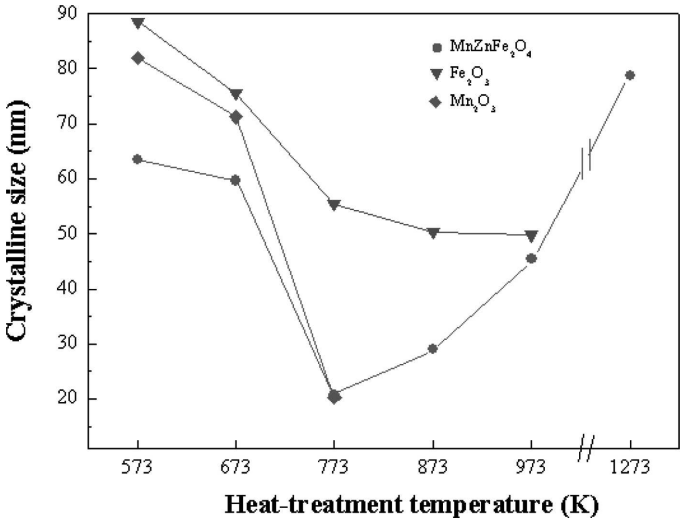

Fig. 6. Crystalline size change of Fe_2O_3, Mn_2O_3 and $MnZnFe_2O_4$ phases with increasing heat-treatment temperature

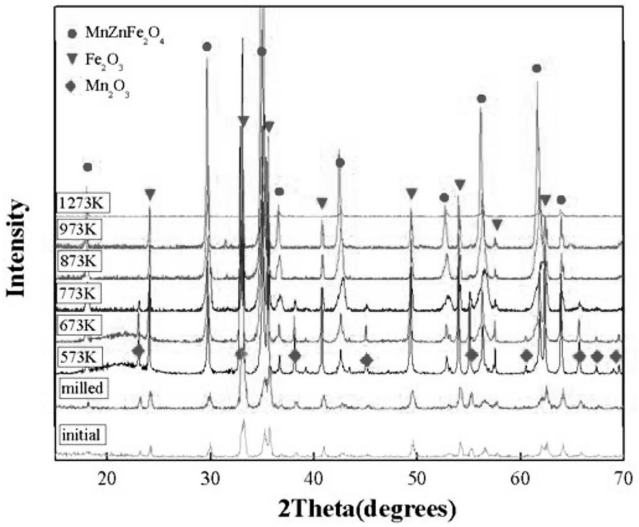

Fig. 5. XRD patterns of the initial, milled and heat-treated ferrite powders

Fig. 7 shows (a) M-H loops, (b) coercivity and saturation magnetization of the initial, milled powders and heat-treated powders. As the heat-treatment temperature increased, the peaks of M-H loops had a tendency to increase, indicating the increase of saturation magnetization as shown in Fig. 7(b). It could be understood that the increase of saturation magnetization is attributed to the continuous growth and formation of $MnZnFe_2O_4$ phase and decomposition of Fe_2O_3 and Mn_2O_3 phases. On the other hand, the powders showed the highest coercivity at 773K and it decreased again with increasing heat-treatment temperature. This can be explained by the change in crystalline size of $MnZnFe_2O_4$ phase shown in Fig. 6 because it is generally known that the coercivity strongly depends on the crystalline size [11].

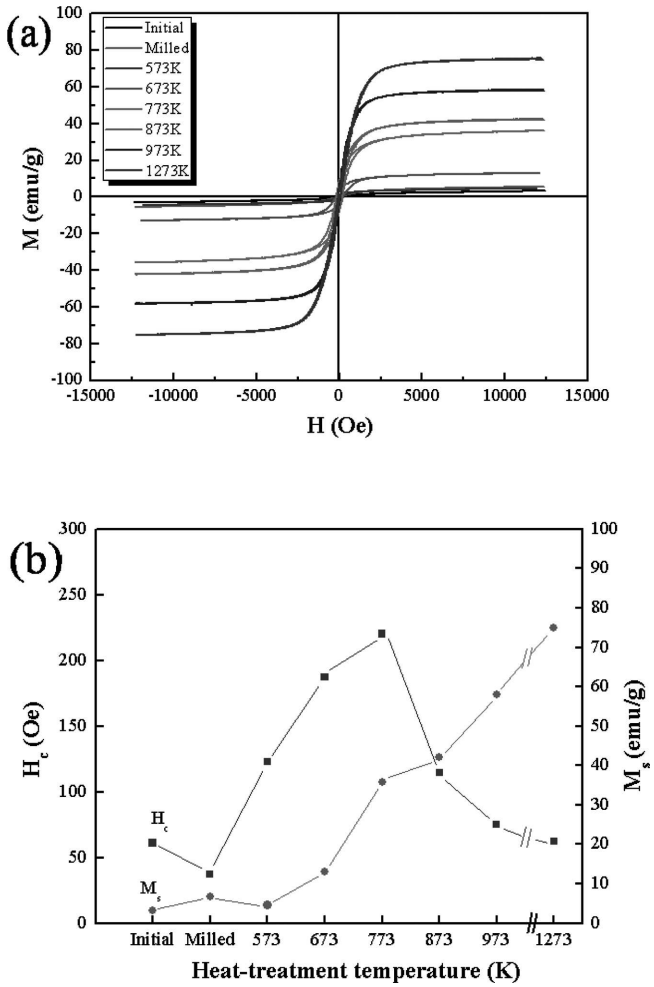

Fig. 7. M-H loops (a) and coercivity (H_c) and saturation magnetization (M_s) (b) of the initial, milled and heat-treated ferrite powders

4. Conclusions

The ferrite powders consisted of Mn_2O_3, Fe_2O_3 and $MnZnFe_2O_4$ phases showed the size of approximately 230nm after milling at 300rpm for 3h. The milled powders included the agglomerated particles with the size of approximately 15nm. The sizes of the powders and agglomerated particles increased to approximately 550nm and 120nm, respectively after heat-treatment at 973K. When the heat-treatment temperature increased, the Mn_2O_3 and Fe_2O_3 phases decomposed at 873K and 1273K, respectively and the only $MnZnFe_2O_4$ phase was detected at 1273K. The saturation magnetization of the powders increased with increasing heat-treatment temperature due to the formation of $MnZnFe_2O_4$ phase and the decomposition of Mn_2O_3 and Fe_2O_3 phases. However, the change of coercivity with increasing temperature well corresponed to the change of crystalline size in $MnZnFe_2O_4$ phase.

Acknowledgements

This work (Grants No.C0002466) was supported by Business for Cooperative R&D between Industry, Academy, and Research Institute funded Korea Small and Medium Business Administration in 2013.

REFERENCES

[1] J. Zhang, Liming Yu, S. Yuan, S. Zhang, X. Zhao, J. Magn. Magn. Mater. **321**, 3585-3588 (2009).
[2] Ping Hu, Hai-bo Yang, De-an Pan, Hua Wang, Jian-Jun Tian, Shen-gen Zhang, Xin-feng Wang, Alex A. Volinsky, J. Magn. Magn. Mater. **322**, 173-177 (2010).
[3] M.M. Hessien, M.M. Rashad, K. El-Barawy, I.A. Ibrahim, J. Magn. Magn. Mater. **320**, 1615-1621 (2008).
[4] D.J. Kim et al., Korean Powder Metallurgy Inst, Powder metallugy & Particulate Materials Processing, Seoul 2010.
[5] S.K. Pradhan, S.Bid, M. Gateshki, V. Petkov, J. Mater. Chem. Phys. **93**, 224-230 (2005).
[6] S. Dasgupta, J. Das, J. Eckert, I. Manna, J. Magn. Magn. Mater. **306**, 9-15 (2006).
[7] S.J. Park, Y.S. Song, K.S. Nam, S.Y. Chang, J. Kor. Powd. Met. Inst. **19**, 122-126 (2012).
[8] S.M. Hong, E.K. Park, K.Y. Kim, J.J. Park, M.K. Lee, C.K. Rhee, J.K. Lee, Y.S. Kwon, J. Kor. Powd. Met. Inst. **19**, 32-39 (2012).
[9] H.P. Klug, L.E. Alexander, Joohn Wiley and Sons, X-ray Diffraction Procedures for Polycrystalline and Amorphous Materials, New York 1997.
[10] L. Zhao, H. Yang, L. Yu, Y. Cui, X. Zhao, B. Zou, S. Feng, J. Magn. Magn. Mater. **301**, 445-451 (2006).

Received: 20 November 2014.